

A Tutorial on Analysis Techniques for Deriving Mechanical Shock and Vibration Environmental Specifications from Field Data

Jerome S. Cap
Sandia National Laboratories*
Albuquerque NM 87185

ABSTRACT

There is a wide variety of applications that subject systems to mechanical shock and vibration environments. How to best characterize those environments and generate the necessary system and component test specifications varies according to the nature of the underlying environment. The purpose of this paper is to provide the reader with an overview of some commonly used analysis techniques for a range of field environments including transportation and handling, aircraft carriage, and missile flight. The paper will also address statistical methods for defining the Maximum Predicted Environment and test control methods as they pertain to achieving the best possible system and component laboratory simulations.

KEYWORDS

Vibration, Shock, Random , Sinusoidal, Specifications

INTRODUCTION

Virtually every time a system moves, it experiences mechanical shock and vibration excitation. The intensity and spectral content of each environment depends on the type of system and the type of motion. This variety presents the analyst with the challenge of identifying 1) the tests and/or analyses best suited to measure input and response data at points of interest, 2) whether the data exhibits any anomalous content, 3) the appropriate spectral analysis, and 4) what is the best means of turning response data into a useful set of laboratory test specifications.

No paper can address every aspect of such a broad topic. Therefore, the purpose of this paper is to present a set of techniques that an analyst can consider using to create a credible set of test specifications. To keep the scope of this paper manageable, the focus will be on experimentally based specifications and single axis test specifications. However, some comments will be made on analytically derived responses and multi-axis system testing.

The references identified in this paper represent applied examples of the concepts described in this paper. A complete list of the papers associated with these topics would be exhaustive, so the reader is encouraged to refer to the references in these papers to gain a more in depth understanding of the underlying theories.

OVERVIEW OF FIELD ENVIRONMENTS

This paper will focus on the mechanical shock and vibration environments associated with ground and air cargo transportation, captive carry flight, and missile flight. However, this paper will be organized according to the temporal and spectral content rather than by the actual source of the excitation.

* Sandia National Laboratories is a multi-mission laboratory managed and operated by National Technology and Engineering Solutions of Sandia, LLC., a wholly owned subsidiary of Honeywell International, Inc., for the U.S. Department of Energy's National Nuclear Security Administration under contract DE-NA0003525.

- 1) Random vibration
- 2) Sinusoidal vibration
- 3) Mixed random and sinusoidal vibration
- 4) Transients and shocks
- 5) Mixed shock and vibration

RANDOM VIBRATION

There are many events for which the environment is almost totally comprised of random vibration. Two common examples include: 1) aircraft captive carry, and 2) the portions of powered missile flight associated with transonic and maximum dynamic pressure (max Q). Figure 1 presents examples of the acceleration waveforms associated with each of these environments.

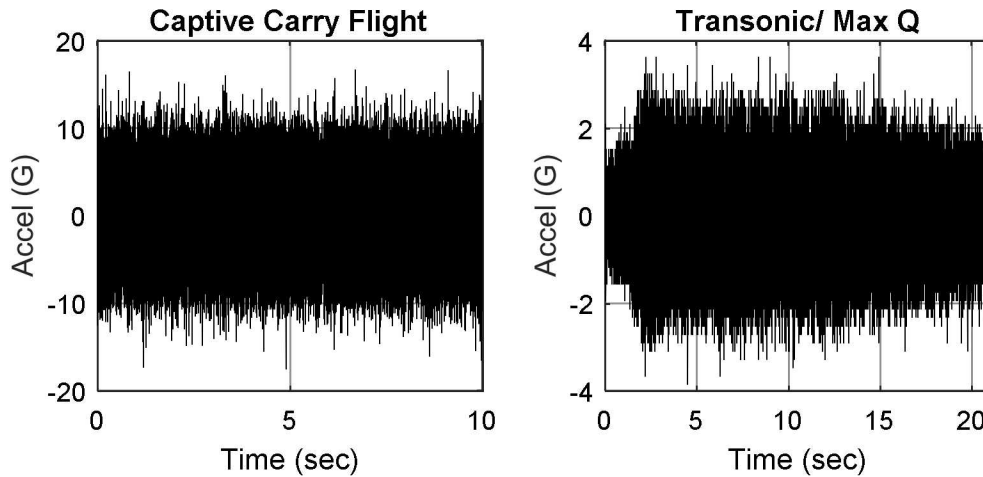


Figure 1: Examples of Random Vibration Environments

A random vibration waveform should be Gaussian or nearly Gaussian. A simple first order check for Gaussian content is to compute the Kurtosis, K , as shown in Equation (1). For a perfectly Gaussian waveform $K=3$. For the captive carry waveform in Figure 1 the Kurtosis is 3.05. For transient waveforms such as the transonic/max Q waveform in Figure 1 one should compute the Kurtosis using a sliding window.

$$K = \frac{\frac{1}{n} \sum_{i=1}^n (x_i - \bar{x})^4}{\left(\frac{1}{n} \sum_{i=1}^n (x_i - \bar{x})^2 \right)^2} \quad (1)$$

The most common means of presenting the spectral content is an Auto-Spectral Density (ASD) or in the case of a Multiple Input, Multiple Output (MIMO) system a Spectral Density Matrix (SDM). While there are several ASD estimators, Welch's Method [1] is perhaps the most common. The ASD analysis parameters include: sample rate (SR), block size (BS), overlap percentage, and window type. The analyst must select the block size that produces the desired frequency resolution ($\Delta f = SR/BS$), while ensuring that an adequate number of analysis blocks are used in the spectral density computation to ensure the desired Normalized Variance Error, NVE. Equation (2) presents the basic estimate of the normalized variance error as a function of the number of blocks, M , used in the ASD estimate.

$$NVE = 1/\sqrt{M} \quad (2)$$

A common estimate of the uncertainty in an ASD is $1 \pm 2 * NVE$. Figure 2 shows how the NVE is related to the "hash" in an ASD and how using more blocks improves the ASD estimate. The analyst must decide how accurate they need the ASD to be

and hence how many blocks of data should be used. Given a limited amount of data the trade-off is between frequency resolution and NVE. Later in this paper the concept of using octal bandwidth ASDs to reduce variance error will be discussed.

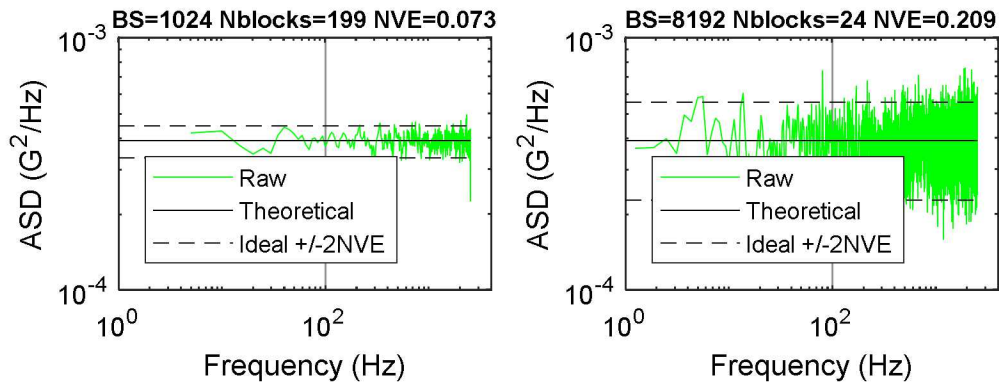


Figure 2: Example of Normalized Variance Error for Two Different Number of Analysis Blocks

Using overlapped blocks can help reduce the NVE, but the reader should note that overlap percentages greater than 50% yield diminishing returns on the effective number of blocks, M_{EFF} , that should be used in Equation (2). The relationship between the raw and effective number of blocks [2] depends on the window used in the analysis and the fraction of overlap. Figure 3 presents this graphically for a Kaiser window with $\alpha=3$. Increasing the fractional overlap increases the number of blocks and hence the raw NVE keeps getting better. However, the effective number of blocks and the corresponding NVE reach an asymptote (the steps in the curve indicate the incremental increase in the number of blocks).

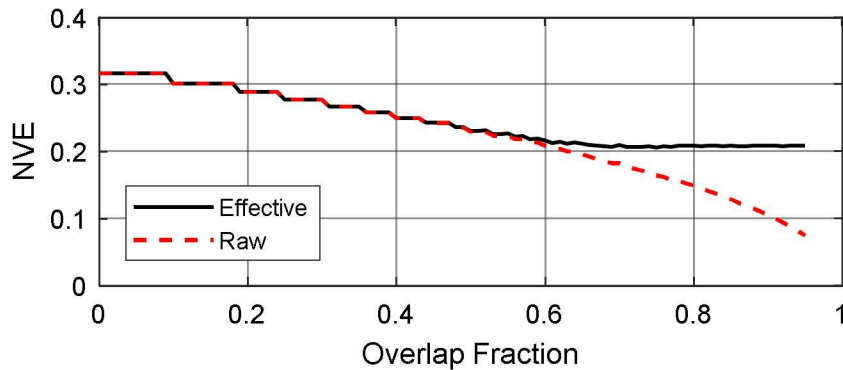


Figure 3: Normalized Variance Error Versus Overlap Fraction (Kaiser Window, $\alpha=3$)

While the initial estimate of the spectral density will have a linear bandwidth frequency resolution, linear bandwidth ASDs are often hashy due to a high NVE, which is an artifact of insufficient data for computing the ASD. One good approach for reducing the variance error is to re-average the ASD using 1/N-th octave frequency bands. This author recommends 1/6th octave bands in keeping with the best practices described in NASA7005 [3], although the original paper on the topic [4] tied the bandwidth to the system damping in order to achieve a balance between the reduction in variance error with the bias error (i.e., the inadvertent rounding off of the peak and valleys associated with the true structural dynamic response). Figure 4 presents an example of a linear and 1/6th octave ASD for the captive carry waveform shown in Figure 1. The reader will note that the hash in the linear ASD is not present in the 1/6th octave ASD.

When displaying an ASD, the analyst should always provide the root mean square acceleration (Grms) since this is the best means of interpreting the general intensity of the environment.

If the random vibration waveform is non-stationary, then the analyst must account for the effects of the non-stationarity on the spectral density estimate. One common technique is a Maxi-Max analysis. For a Maxi-Max analysis, the random vibration waveform is divided into segments and an ASD is computed for each segment. The segments can be overlapped using whatever percentage the analyst deems necessary to capture the time-varying nature of the environment.

How to best interpret the ensemble of Maxi-Max ASDs depends on how the analyst intends to use the results. For example, using the envelope of the ensemble of ASDs is best for insuring that any subsequent test specification is conservative. However, applying the envelope for the entire duration of the event could lead to excessive fatigue damage. The alternative is to use a fatigue damage model to either reduce the magnitude of the composite ASD and/or adjust the effective duration of the event until the resulting combination of level and duration produces the same fatigue damage as the underlying transient environment. Figure 5 presents the ensemble of 1/6th octave Maxi-Max ASD for the transonic / max Q waveform shown in Figure 1 along with the underlying ensemble of individual ASDs.

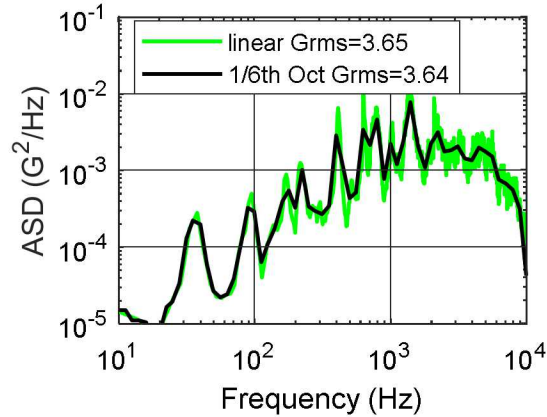


Figure 4: Captive Carry Environment Linear and 1/6th Octave Bandwidth ASDs

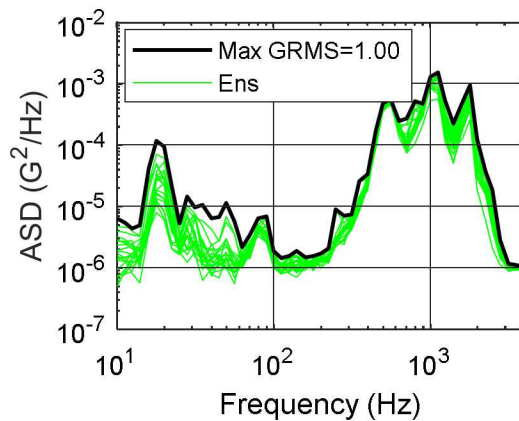


Figure 5: Missile Transonic / Max Q Flight Ensemble of 1/6th Octave Bandwidth ASDs

SINUSOIDAL VIBRATION

Not counting rotating machinery, there are few pure sinusoidal environments, but perhaps the one that is potentially every bit as damaging as any random vibration environment is the swept sinusoidal environment associated with rocket motor resonant burn.

A good technique for analyzing sinusoidal data is the Waterfall Spectrum (WFS). A WFS is simply a series of Fourier Transforms (FTs) computed for windowed blocks of overlapped data. The resulting FT magnitudes can be scaled to produce the correct peak amplitude for a known sinusoidal input.

If the frequency and amplitude of the waveform are changing rapidly with time, the analyst can consider overlapping the analysis blocks to achieve finer time resolution. One can also zero pad the windowed blocks of data to achieve finer frequency resolution. Figure 6 presents an example of a motor resonant burn acceleration waveform and the resulting WFS.

The envelope of the WFS for all time (denoted as a Waterfall Profile or WFP) can be used directly to define a laboratory swept sine test. The “ridgeline” of the WFS can be used to define the sweep rate. Figure 7 presents the WFP and ridgeline for the WFS shown in Figure 6.

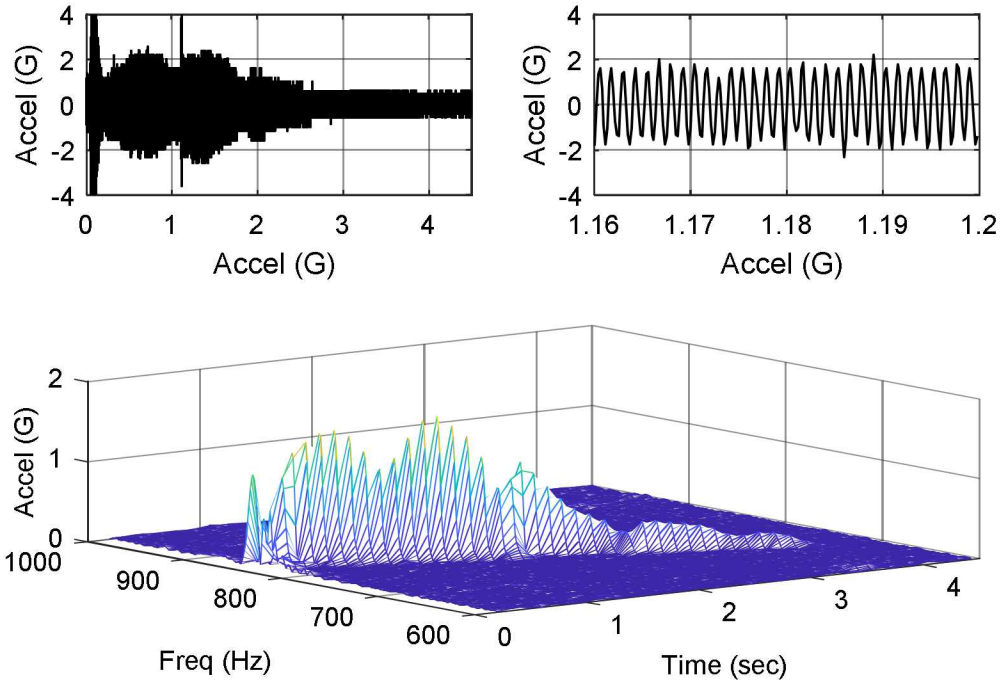


Figure 6: Example of WFS for a Motor Resonant Burn Swept Sinusoidal Environment

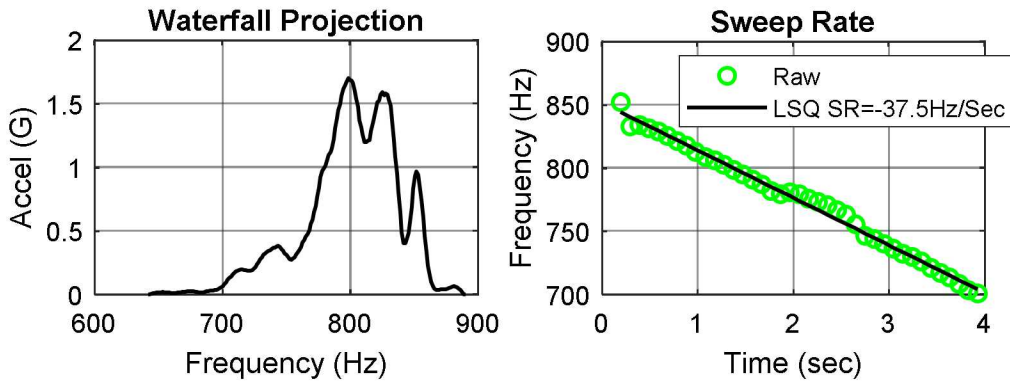


Figure 7: Example of WFP and Sweep Rate Estimate for a Motor Resonant Burn Swept Sinusoidal Environment

MIXED RANDOM AND SINUSOIDAL VIBRATION

Air transportation environments involving turboprop aircraft and helicopters contain a mixture of random and sinusoidal vibration. Sometimes what at first appears to be sinusoidal content can in fact be narrowband random. The least bit of shift in the RPMs associated with a multi-engine turboprop aircraft can result in a modulated nearly sinusoidal waveform that starts to look like a narrowband random waveform. A simple way to determine if a waveform is sinusoidal or narrowband random is to plot a histogram of the peaks for a bandpass filtered version of the waveform. The peaks for an ideal narrowband random waveform will follow a Rayleigh distribution whereas the peaks for an ideal sinusoidal waveform will have a constant amplitude. Many real-world waveforms fall somewhere in between these two ideal cases. Figure 8 presents an example of mixed sine on random vibration data (actually 60 Hz noise).

The key to analyzing a true sine-on-random content environment is to separate the sinusoidal content from the broadband random content. The separation can be done in the time domain by estimating the amplitude and frequency of the sinusoid and then subtracting that content from the raw waveform. In the frequency domain either ASDs or WFS can be used to identify

the magnitude of the sinusoidal content and then the corresponding spikes can be edited out to leave an estimate of the broadband random content.

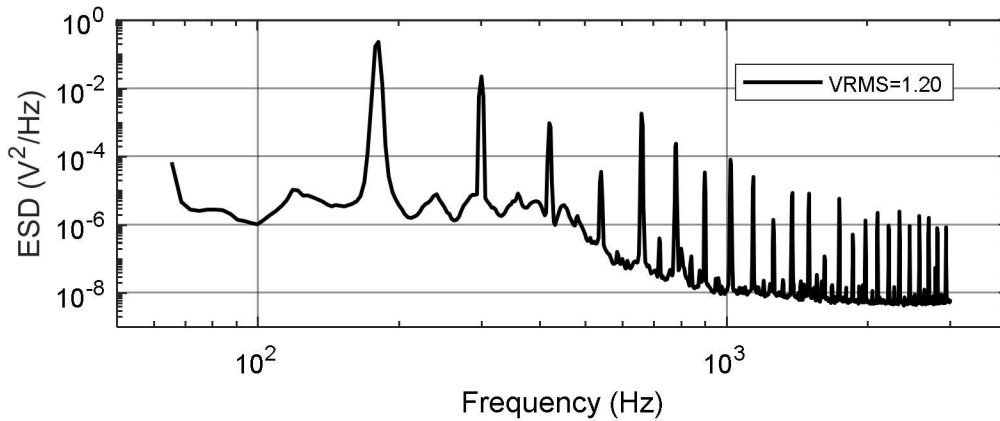


Figure 8: Example of Sine on Random Vibration Environment

TRANSIENTS AND SHOCKS

When an environment is too short to analyze using spectral densities, the analyst must start treating the environment as a shock. Events that fall into this category include: 1) missile launch transients, 2) pyrotechnically induced separation shocks, and 3) ground impact shocks. Figure 9 presents acceleration waveforms for each of these environments.

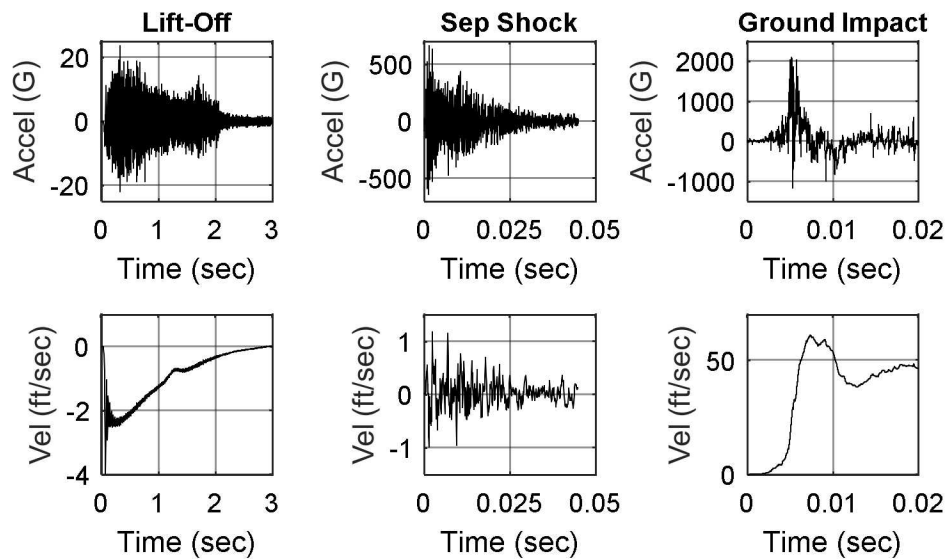


Figure 9: Temporal Waveforms for Launch, Stage Separation, and Ground Impact Environments

The most common means of characterizing the spectral content of a shock environment is the Shock Response Spectra (SRS) or the Pseudo Velocity Response Spectra (PVRS). Fourier Energy Spectrum (FES) and Input Energy Spectrum (IES) [5] are also used. SRS, PVRS, and IES all use Single Degree of Freedom (SDOF) oscillators to characterize the spectral content of the shock. In each case the analyst chooses the resonant frequencies of the SDOF oscillators (a minimum of 1/12th octave resolution is recommended) and the damping of the SDOF oscillator (in theory the damping should be set equal to the anticipated system damping but from a practical perspective values in the 3-5% range are typically used).

In the interest of brevity, this paper will focus on SRS. The SRS presented in this paper were computed using a Maxi-Max Absolute Acceleration (MMAA) algorithm with a 3% of critical damping ratio. Figure 10 presents the SRS for the environments shown in Figure 9 (the damping ratios for these SRS varied so they are identified in the legends).

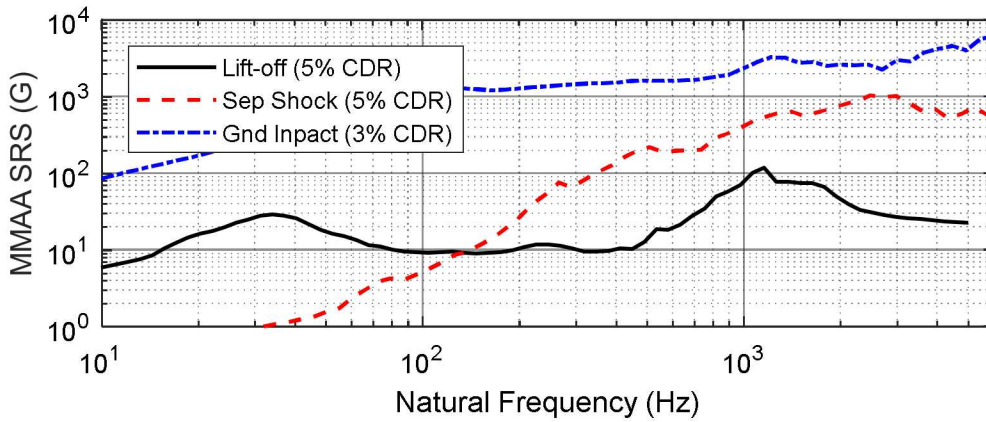


Figure 10: SRS for Launch, Stage Separation, and Ground Impact Environments

MIXED SHOCK AND VIBRATION

Perhaps the main feature of ground transportation environments is the fact that mechanical shocks of varying intensity are intermixed with quasi-stationary vibration. The upper plot in Figure 11 presents an example of acceleration response data for a truck transportation road test.

The analyst must decide how to parse the data. One useful approach is a skyline plot. A skyline plot, like the one shown in the lower plot in Figure 11, is simply a set of one or more metrics (peak G, rms G, Kurtosis, etc.) computed using sequential blocks of data. The analyst must choose the duration and overlap of the blocks to capture each shock event in a single block while not zooming out so far as to include significant random vibration content in with the shocks. The analyst should review every shock to avoid including electrical noise spikes and to look for signs of over-ranged accelerometers (the temptation with the large file sizes associated with transportation environments is to totally automate the process).

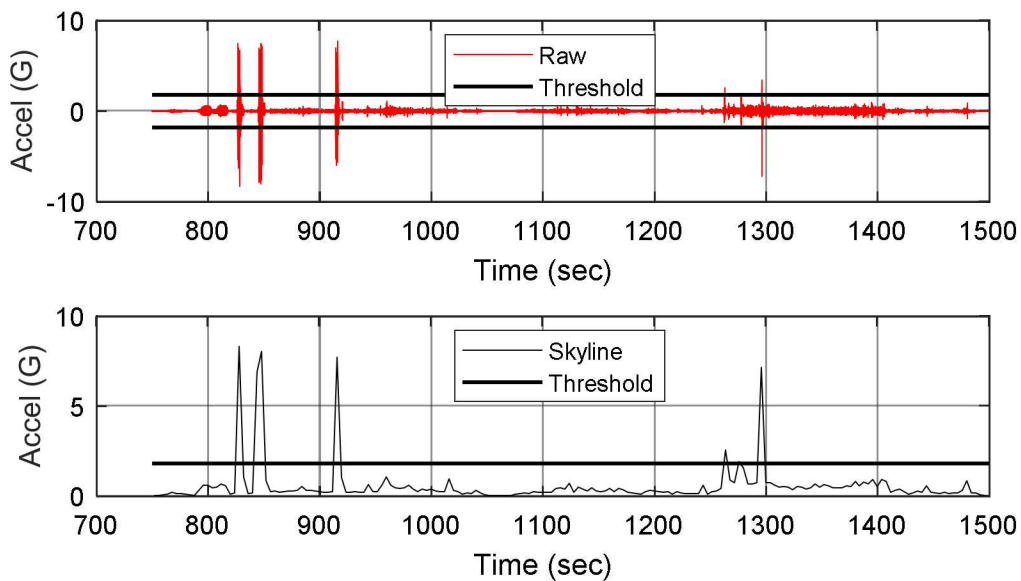


Figure 11: Truck Transportation Acceleration and Skyline Data

The analyst must also choose the threshold between shocks and vibration based on the character of the skyline plot. Unless the analyst is trying to establish the complete distribution of shocks, it is probably better to include a few low-level shocks in with the vibration environment rather than including vibration events in with the shocks.

All blocks that include shocks are extracted for analysis using a model such as SRS. Adjacent “shock” blocks should be concatenated (making sure to not double count overlapped portions) since they most likely are catching the same shock event. All blocks that include only vibration are concatenated (again making sure to not double count overlapped portions) and analyzed using ASDs. Figure 12 presents ensembles of ASDs and SRS for the acceleration waveform defined in Figure 11.

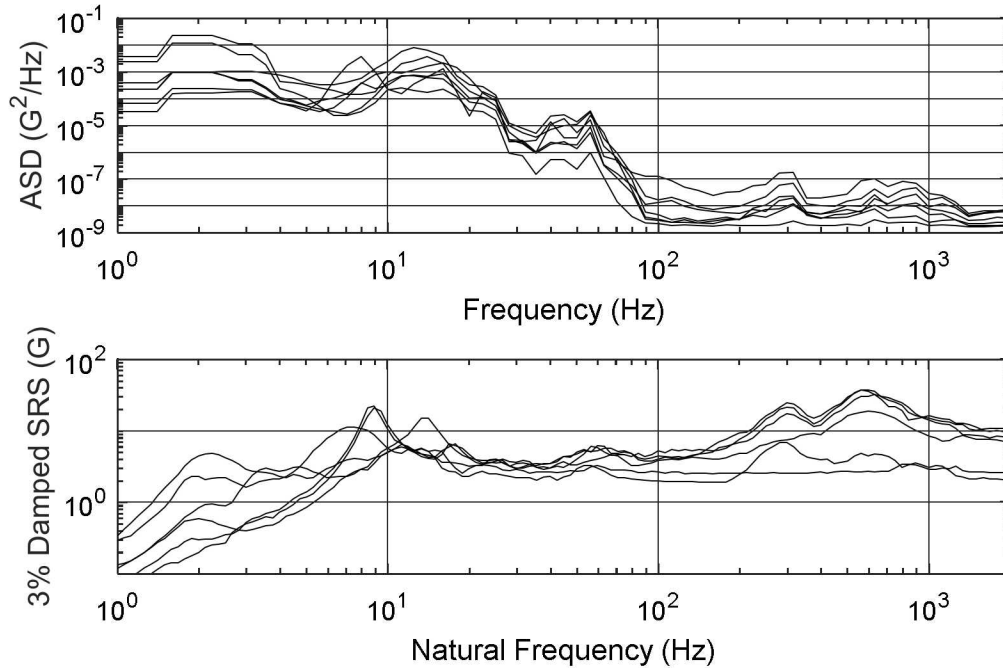


Figure 12: ASD and SRS Ensembles for the Mixed Shock and Vibration Truck Transport Environment

BEST PRACTICES FOR MEASURING GOOD DATA DURING FIELD TESTS

An important part of developing good test specifications is acquiring good data from the next assembly level tests and/or analyses. Acquiring good field data starts well before the test begins.

The analyst should use available knowledge about the intensity and spectral content of the field environment when choosing their transducers (typically accelerometers). The data acquisition system (DAS) should have good anti-aliasing filters and a sufficiently small bit resolution for the desired accuracy. A good rule of thumb for the digital noise floor of the DAS is ½ bit. Equation (3) generates the bit resolution, G_{BR} , as a function of the number of bits, N , in the analog to digital converter (ADC) and the total amplitude range of the ADC, $Grange$. Equation (4) computes the theoretical noise floor ASD, S_{TNF} , where f_N is the Nyquist frequency (1/2 of the sample rate).

$$G_{BR} = Grange / (2^N - 1) \quad (3)$$

$$S_{TNF} = (G_{BR} / 2)^2 / f_N \quad (4)$$

Sigma-Delta ADCs tend to be better than traditional ADCs, but they can be mis-applied.

Where possible, a noise transducer should be employed to identify whether spurious responses represent real mechanical response or electrical noise. Another good practice is to acquire a data set without any external stimulation to establish the noise floor of the DAS.

Lastly, independent measures of critical parameters are often useful. For example, using photometrics or laser displacement sensors to capture the rigid body response of a system can come in handy when assessing the accuracy of the accelerometers used on a test and can possibly be used to correct the low frequency response from piezoelectric accelerometers (since they cannot accurately measure rigid body acceleration).

DATA QUALITY CHECKS

During the post-test review, the analyst should view data with a skeptical eye. The velocity is an excellent check on the credibility of any acceleration measurement. For tests in which the net velocity should be zero, any drift in the accelerometers represent potential error (small offsets in the acceleration data can usually be removed without fear that the remaining trace is bad). The anomalous acceleration data can be removed using techniques such as high pass filtering or curve fitting the anomalous content (this latter approach works better on the velocity waveform).

Spikes that can be traced to electrical noise (such as cross talk between the fire pulse and the accelerometer cables during a live fire pyrotechnic test) and/or content associated with 60 Hz line noise and its harmonics should also be removed.

STATISTICAL MODELING

Most field tests have inherent test-to-test variability. Therefore, it is prudent to employ statistical models to define a Maximum Predicted Environment (MPE). The MPE should have a stated probability of occurrence and confidence interval.

Statistical models require multiple data sets measured under nominally the same conditions. For events such as captive carry this rarely happens. However, parametric models can be used to merge data from nominally different flight conditions if one understands the relationship between the parameters and the response data. For example, References [6] and [7] document the relationship between dynamic pressure, Q , and the rms vibration response for the turbulent boundary layer flow associated with external captive carry. Figure 13 presents such a scaling model [8].

The upper plot shows an ensemble of as-measured ASDs, while the middle plot shows the linear relationship between Q and Grms for the raw ASDs, as well as the resulting Grms values scaled to the desired value of Q (the difference between the measured Grms values and the linear fit is assumed to represent the flight to flight variability). Equation (5) describes the scaling model. The bottom plot shows the resulting scaled ASDs where m_{MN} is the slope and b_{MN} is the y-intercept. The reader can see that the spread in the data is reduced, which generally results in a lower prediction of the MPE.

$$G = m_{MN}Q + b_{MN} \quad (5)$$

Another common parametric model is used when data comes from systems having somewhat different geometries but essentially the same forcing functions. The resulting ensembles of response spectra will have similarities but also marked differences. The assumption is that the differences are described by the means for each system while the flight to flight variation is independent of which system was being flown. The technique for merging the two ensembles, $S_{ENS(A)}$ and $S_{ENS(B)}$, is a form of regression bootstrapping. Equations (6) and (7) are used to separate each ensemble into its respective mean, S_{MN} , and difference, S_{DIF} . Equation (8) shows how the sets of differences for both ensembles are added to the mean for ensemble B to create a composite ensemble, $S_{ENS(CMP)}$. Figure 14 shows an example of this technique applied to a bifurcated ensemble based on 16 nominally identical tests performed on the same test unit (the analysis was conducted on the log of the data).

$$S_{DIF(A)} = S_{ENS(A)} - S_{MN(A)} \quad (6)$$

$$S_{DIF(B)} = S_{ENS(B)} - S_{MN(B)} \quad (7)$$

$$S_{ENS(CMP)} = S_{MN(B)} + [S_{DIF(A)}, S_{DIF(B)}] \quad (8)$$

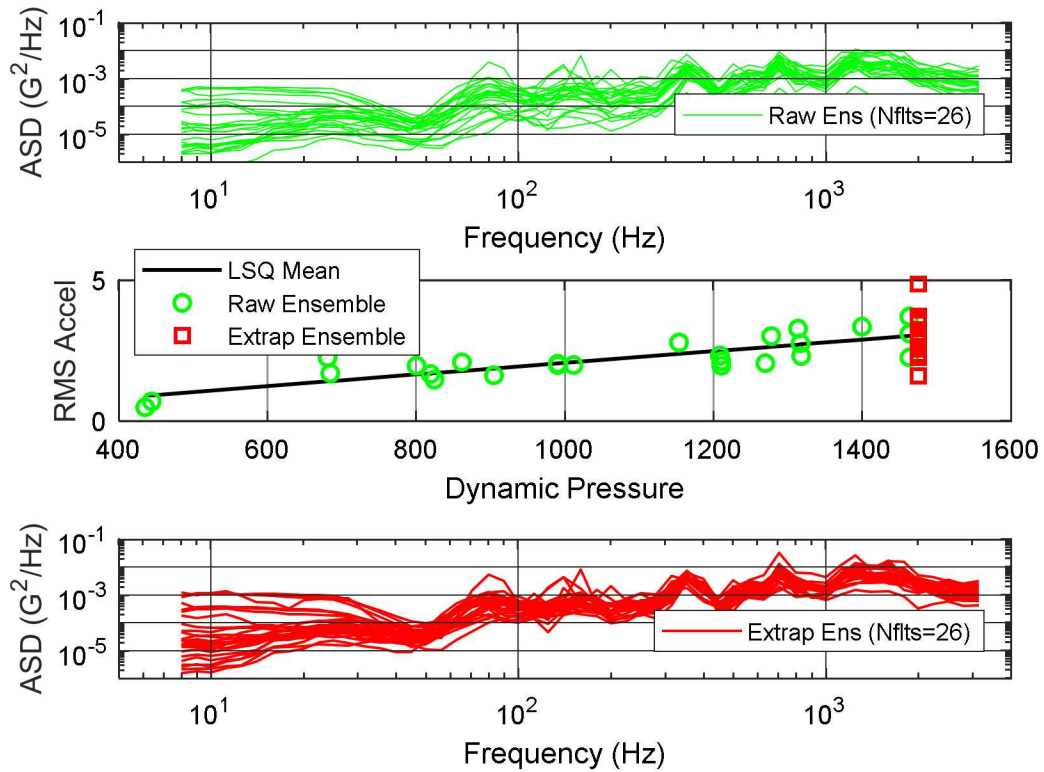


Figure 13: Example of Q Scaling Model for External Captive Carry Flight Vibration

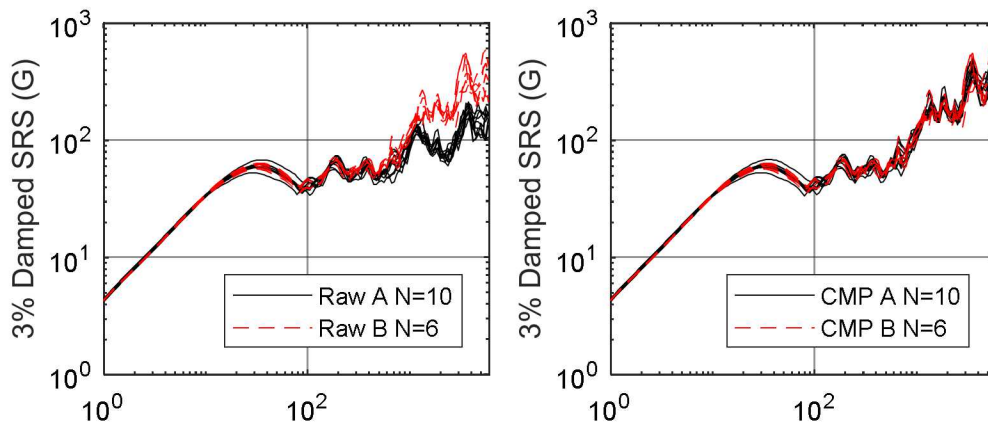


Figure 14: Example of Merging Bifurcated Data Ensembles

Once the analyst has compiled a homogeneous ensemble of data, the next step is to choose the best statistical model. When sufficiently large data sets are available, the analysts can simply rank order the results and choose the spectrum (one frequency at a time) associated with the desired probability of occurrence. This approach is referred to as a Distribution Free Tolerance Limit (DFTL) or Empirical Tolerance Limit (ETL).

When the available data set is small, but there is evidence in support of a closed form analytical model, such as a normal or lognormal distribution, the solution becomes straightforward. Equation (9) presents the Normal Tolerance Limit (NTL) formulation presented in NASA7005 for computing the MPE estimate for a desired probability, P , and confidence, C , $X_{P/C}$

based on the mean (μ) and standard deviation (σ) of the raw ensemble [3]. There are both lookup tables and analytical models [9] for computing the value of k as a function of the number of flights and the desired probability and confidence.

$$X_{P/C} = \mu + k\sigma \tag{9}$$

The value of k becomes quite large for small numbers of spectrum to account for uncertainty in the estimates of the mean and standard deviation.

For small sample sizes (3-5), SMC-TR-06-11 [10] proposes that the user assume a standard deviation, σ , of 3dB, thereby avoiding the adjustment in the NTL model associated with small sample sizes. Equation (10) presents this formulation for computing a scale factor, $L_{P/C}$, to be applied to the logmean of the data for the desired probability, P , and confidence, C , given the number of flights, N . For the P99/90 scale factor, $Z_P=2.322$ and $Z_C=1.282$.

$$L_{P/C} = \sigma(Z_P + Z_C/N^{1/2}) \quad (\text{dB}) \tag{10}$$

Figure 15 compares the dB scale factors relative to the sample means for the NASA7005 and SMC (Rubin 1540) models. The reader can see that the SMC and NASA models are identical for large values of N , but the SMC model calls for greatly reduced scale factors for small values of N .

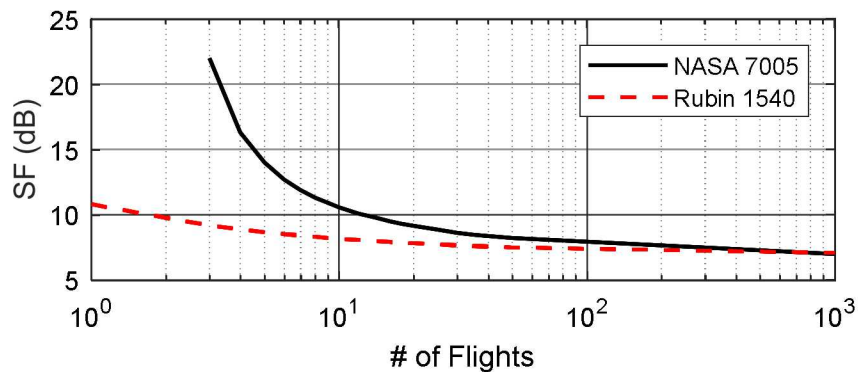


Figure 15: Comparison of NASA and SMC Statistical Models

The reader should understand that the standard deviation used in this model was based on Trident I flight data [11]. Therefore, one should exercise caution when using this formulation for carriers other than launch vehicles.

Principal Component Mode Synthesis techniques such as a Karhunen-Loeve (KL) expansion model [12] fit a set of shape functions (such as Eigenvectors) to the ensemble of spectra and then generate large numbers of realizations by randomly varying the weighting of the shape functions. The analyst then simply ranks the realizations using a distribution free tolerance model and chooses the spectrum having the desired probability of occurrence, P . KL models work very well for ensembles having as few as 5-10 spectra.

Bootstrapping techniques can be used to improve the confidence in a KL model. The bootstrap technique resamples the original data with replacement to help the analyst understand what the MPE results would look like if a different ensemble had been measured in the first place. Generally, many bootstrap runs are conducted and the set of P percentile spectra from each bootstrap run are collected and rank ordered. The spectrum having the desired probability is used to represent that level of confidence in the MPE prediction.

Figure 16 compares the Q scaled ensemble from Figure 13 against the P99/90 MPEs using the KL and NTL algorithms. Since the KL expansion model as defined in [12] uses a Gaussian seed to synthesize realizations it is not unexpected that it agrees with the NTL model for a relatively large ensemble size like the one used in this example.

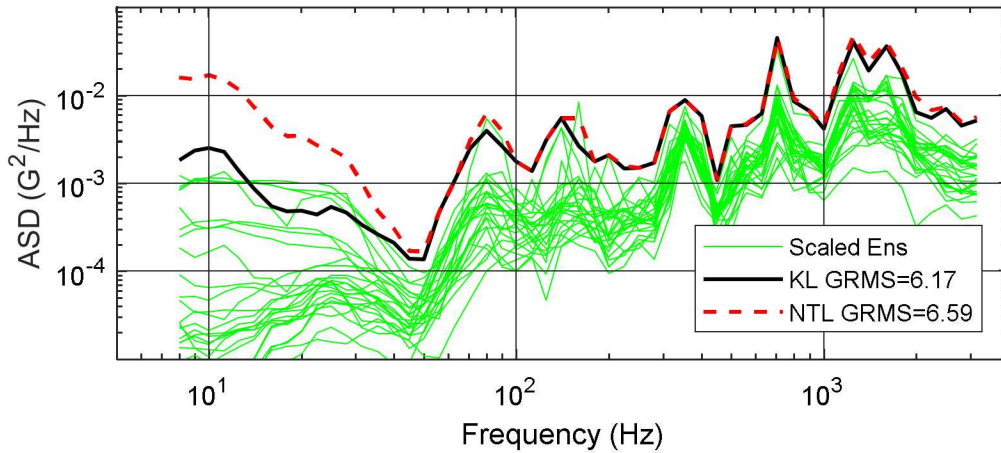


Figure 16: Example of Distribution and P99 Value for 2000 Realizations of an External Captive Carry Environment

DURATION

The final step in defining the MPE environment is establishing the effective duration. For fatigue inducing environments (random vibration, sinusoidal vibration, and multiple hit, low G shocks), the key is to define the anticipated service life and determine whether the intensity of the environment is constant or varies as a function of time. For example, Figure 17 shows the Probability Distribution Function (PDF) of Grms levels for interstate truck transport [13] along with the P99/90 Grms value. Clearly the MPE level is not present for the entire duration of the road trip.

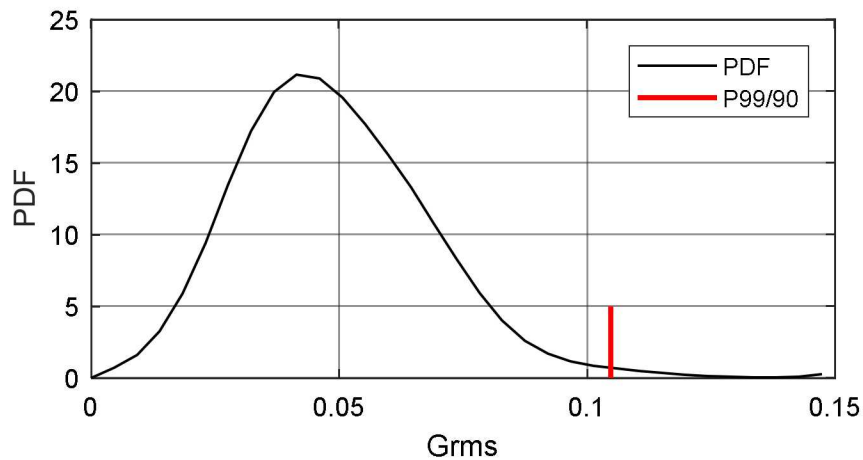


Figure 17: Distribution of Vibration Intensity for an Interstate Road Trip

Captive carry flights have less variation for a given dynamic pressure, but a typical mission profile often includes only a few minutes of max Q flight and many hours of low Q flight associated with high altitude cruise.

In both cases there are two approaches for defining the duration: 1) define a stepped test schedule of levels by dividing the PDF into segments and durations with respect to the MPE levels, or 2) employ a test time compression model such as the Miner-Palmgren power law model shown in Equation (11) to shorten the test duration.

$$D = \sum_{i=1}^n \Delta T_i G_i^b \quad (11)$$

Where ΔT_i and G_i are the distribution of field durations and amplitudes derived from the PDF and b is the fatigue exponent. $1/b$ is the slope of the fatigue stress vs cycles (S-N) curve.

Since raising the levels of the test beyond the MPE levels introduces the possibility of a false failure, it is recommended that the analyst first compress the times associated with the lower magnitude events. For the PDF shown in Figure 17 and a fatigue coefficient of $b=6.65$ (a typical value for a ductile material) a 1000-mile road trip (20 hours) can be replicated with 1 hour of testing at the P99/90 levels. This is consistent with guidance in Mil-Std-810 [6].

For low G , multiple occurrence shocks that produce fatigue damage, the same power law models can be used to estimate how many worst-case shocks must be applied to produce the same damage as the ensemble of field shocks [14].

For high G shocks having only a few occurrences, one can assume that any failures will be due to first passage failure and hence one hit in each direction of concern is theoretically sufficient. However, it is always prudent to apply as many hits as the underlying environment dictates.

CREATING COMPONENT RESPONSES FROM SYSTEM LEVEL LABORATORY TESTS

This section addresses the issues associated with deriving component specifications from system level laboratory tests. Shaker tests (especially single axis setups) rarely can replicate the true field environment owing to differences in boundary conditions and in how the inputs are applied. Multi-axis shaker tests and acoustic tests tend to do better, but even these methods can still fall short. Therefore, the most important thing to understand is how accurate the test is. Figure 18 presents the error associated with three system tests: 1) a MIMO acoustic test simulating missile launch [15], 2) a MIMO vibration test simulating external captive carry flight [16], and 3) a Single-Input-Multiple-Output (SIMO) shaker test simulating captive carry flight [17]. It is useful to have a scalar estimate of the overall error in the ensemble of responses. Equation (12) computes the rms dB error, E_{RMSDB} , based on the sum of the rms dB ratios of the measured spectrum, S_M , divided by the desired spectra, S_R , normalized by the ratio of the k -th frequency bandwidth, $\Delta f(k)$ divided by the total frequency range, f_B . The rms dB error is presented for each ensemble in Figure 18.

$$E_{RMSDB} = \left(\frac{1}{N} \right) \sum_{n=1}^N \left(\sqrt{\frac{\sum_{k=1}^K \left[\left(10 \cdot \log \left(\frac{S(k)_M}{S(k)_R} \right) \right)^2 \Delta f(k) \right]}{f_B}} \right) \quad (12)$$

The SIMO was clearly less accurate than the MIMO tests, which is believed to be due to the limitations in the realism of the forcing function and boundary conditions.

These tests were based on multiple internal responses acquired from field tests. If one does not have the luxury of field data, then the only choice is to try for the best possible replication of the boundary conditions and inputs. In many cases the test engineer is forced to control the test on the shaker table using a generic specification. This latter approach tends to produce overly conservative responses because straight line specifications tend to over excite the fixed base resonant frequencies in the system [18].

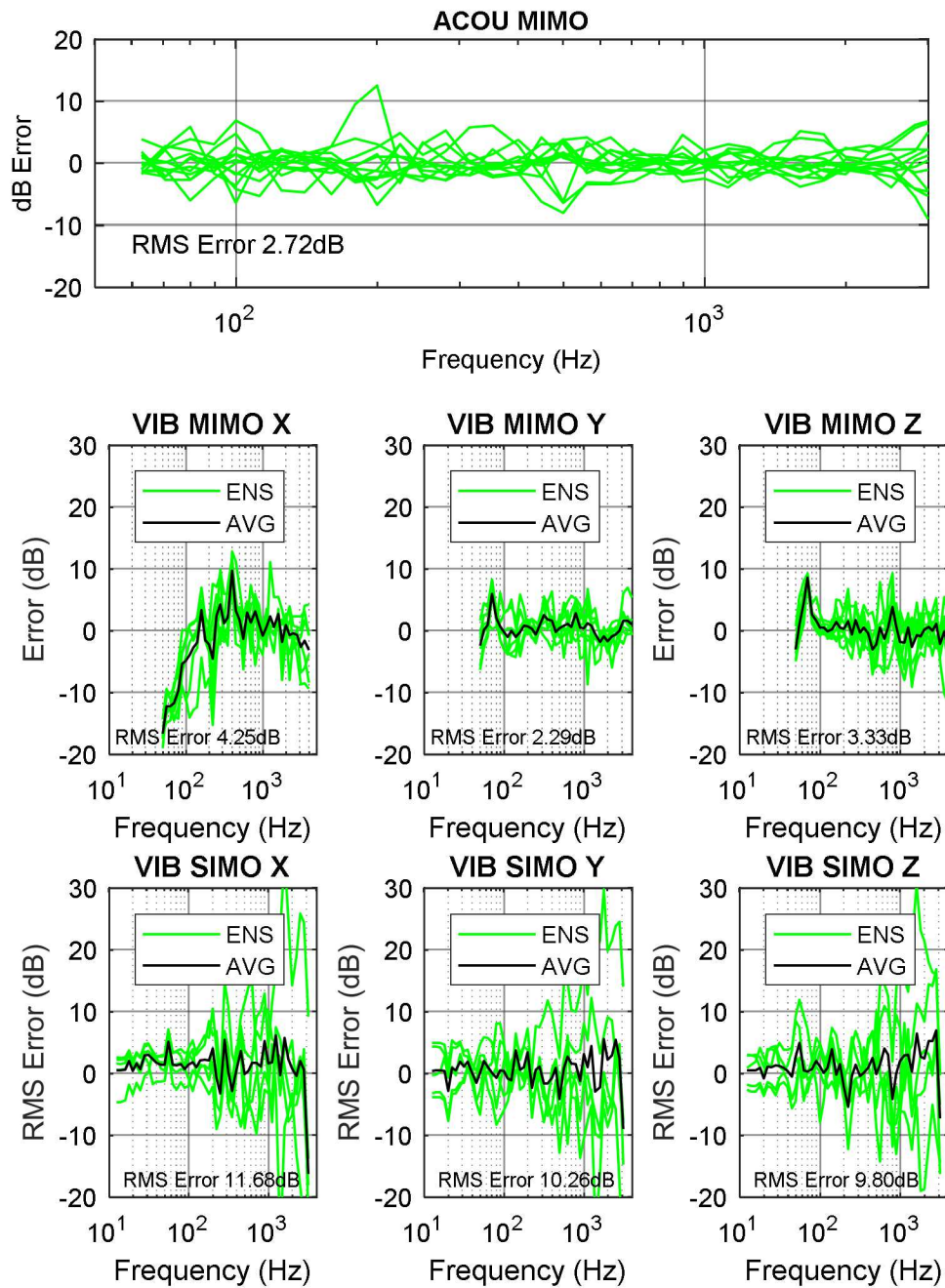


Figure 18: Examples of the Accuracy for Three System Tests

When employing single axis testing, it is recommended that the final component responses be based on some combination of the in-axis and cross-axis responses (i.e., the Y axis response to the X, Y, and Z axis inputs). If the system test is based on a SIMO approach for matching multiple in-axis responses, then the cross-axis responses are simply artifacts of the test and the three responses should simply be enveloped. Conversely, if the system tests consist of three base inputs then one should assume that the cross-axis responses could be real and summing the three responses is recommended. Figure 19 presents an example of the envelope of the in-axis and cross-axis responses for a set of single axis SIMO shaker tests.

The analyst may choose to apply correction factors to data acquired from laboratory tests based on the known accuracy of the setup.

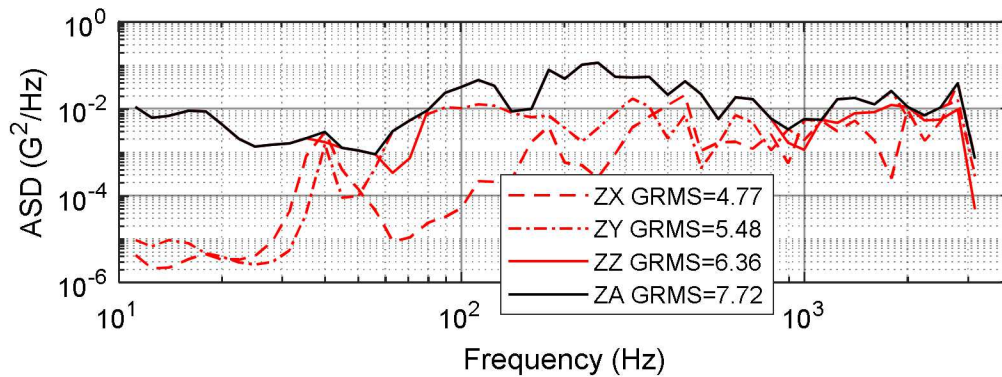


Figure 19: In-Axis and Cross-Axis Responses for Single Axis Shaker Tests

OBTAINING SYSTEM RESPONSES FROM ANALYTICAL MODELS

Finite Element (FE) models have an advantage over laboratory tests since they can better replicate the boundary conditions and inputs associated with the field conditions. Conversely, FE models can have trouble capturing the true internal behavior. Shifts in resonant frequencies and errors in the damping values can adversely affect the accuracy of the model predictions. As was the case for system level laboratory tests, it is desirable to assess the model using field data and potentially make corrections as deemed appropriate.

GENERATION OF SPECIFICATIONS

Given the MPE spectrum, the next step is to develop a practical test specification. Test labs prefer specifications consisting of relatively few straight-line segments. There are pros and cons to such an approach, so the analyst should use good judgment when developing such specifications.

When enveloping the raw MPE spectra one should allow for uncertainty in the MPE spectrum. If the MPE spectrum was based on a high statistical level (such as P99/90) then one does not really need to apply a cushion on the magnitude. However, it is common for field testing to be performed using one or two test assets. Furthermore, the full range of temperature extremes are rarely encountered during a field test. Therefore, including a cushion for left/right shifting of peaks in the MPE spectrum is recommended. If some measure of the variability exists it can be taken advantage of. If no such information is available, then one must use their best judgment. An automated algorithm was developed at Sandia that draws plateaus on top of the peaks in the spectrum and connects the plateaus with ramps. This approach works best with octal banded ASDs. For example, for a 1/6th octave MPE ASD, using 1/3rd octave plateaus allows for 1/12th octave cushions on either side of the peaks in the MPE spectrum. The slope must be achievable in the test lab (24 dB/octave is a reasonable value). Figure 20 presents an example of the enveloping process. The algorithm technically uses the piecewise representation of the ASD, so the analyst must always keep in mind what the corresponding rectangular band version looks like. Both versions of the MPE ASD are provided in this example.

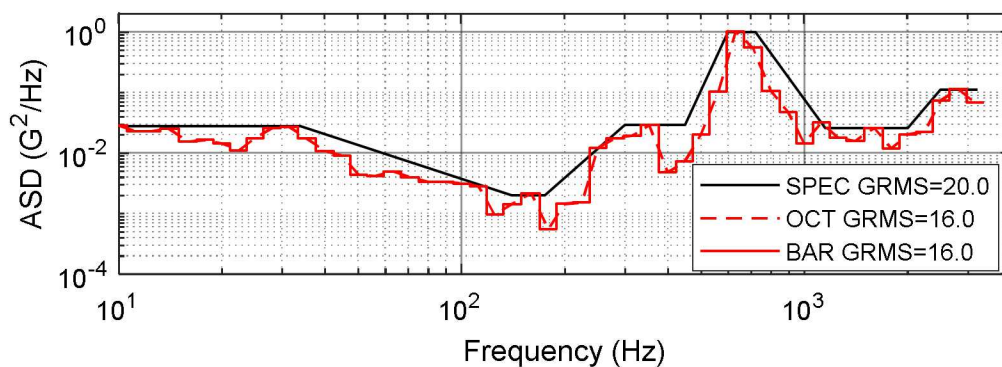


Figure 20: Example of Random Vibration Test Specification & Underlying MPE Spectrum

The final check on a random vibration specification is that the Grms of the specification should not significantly exceed the Grms of the underlying MPE spectrum. A 50% exceedance is on the high end of reasonable.

Applying this type of algorithm to WFPs or SRS does not work quite as well, since those types of spectra tend to have much shallower ramps and less pronounced peaks. The analyst can still use the basic concepts of plateaus and ramps and some measure of the overall increase in the “area under the curve”.

While ASDs and WFPs can be directly implemented in the vibration test lab, shocks require the synthesis of an acceleration waveform whose SRS matches the desired SRS within a given tolerance and meets the limitations of the shaker for acceleration, velocity, and displacement.

Common waveforms used in shock synthesis include 1) sums of decayed sinusoids, 2) half-sine modulated sinusoids (wavelets), and 3) windowed random. The basic algorithms for deriving several types of acceleration waveforms was worked out by David Smallwood [19]. Equation (13) presents the formulation for decayed sine shaker shocks where A_k are the tonal amplitudes, f_k are the tonal frequencies, and ζ_k are the tonal decay rates.

$$A(t) = \sum_{k=1}^N A_k e^{-2\pi\zeta_k f_k t} \sin(2\pi f_k t) \quad (13)$$

The basic parameters used for this example are:

- 1) Sample rate of ≈ 10 times the highest tonal frequency. The minimum recommended oversampling rate is ≈ 5 .
- 2) Duration equal to 8 times the period of the lowest tonal frequency. This allows the lowest tones to have enough oscillations to produce a good SRS analysis.
- 3) The exponential decay rate, ζ , was defined to force the waveform to decay to 5% of the initial peak value. This ensures that the shaker will essentially be at rest at the end of the test.
- 3) 6 tones/octave. While one can often match the desired SRS using as few as 3 tones/octave, using more tones tends to produce a better match for the desired SRS, reduce the peak acceleration, and provide a richer spectral content (the field environment is more likely to be random in content and hence exhibit a broadband spectral content). A Sandia study suggests a minimum tonal density of 4 tones/octave for 5% damped SRS and a minimum tonal density of 6 tones/octave for 3% damped SRS.
- 4) Alternate the polarity of every other tonal amplitude. This tends to produce a smoother SRS.

Figure 21 presents an example of a waveform constructed using sums of decayed sines.

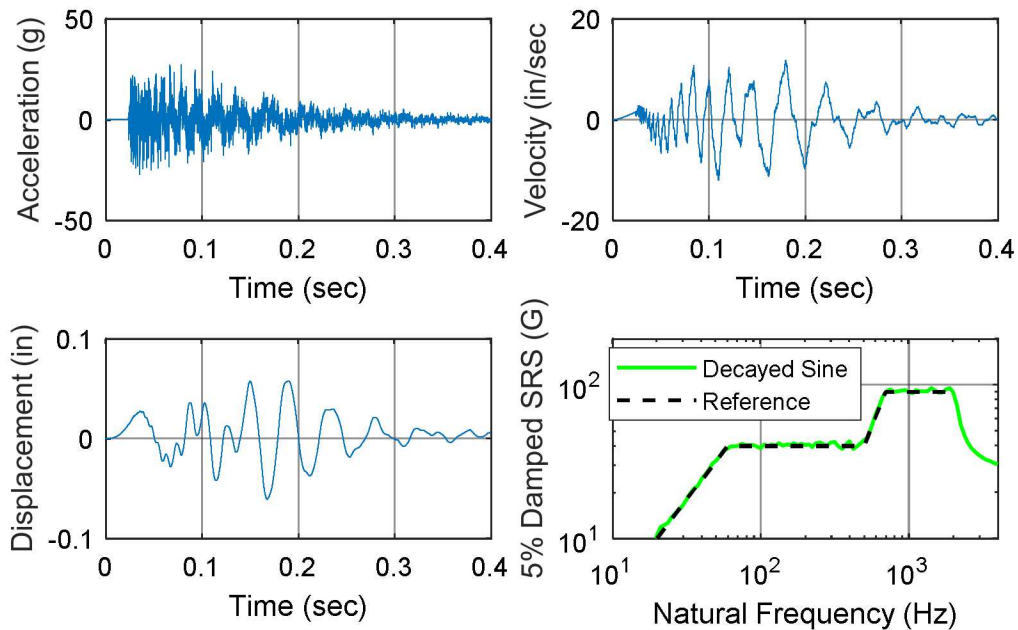


Figure 21: Example of Decayed Sine Shaker Shock

GENERATION OF COMPOSITE SPECIFICATIONS

The next topic is the combining of several specifications to reduce the number of unique tests. Component designers (and sometimes test engineers) often request this to save time and money. It is the job of the analyst to make sure that the resultant specification does not represent an over or under test. Therefore, how to handle this depends on the classes of specifications being combined.

For shocks that are assumed to produce first passage failure, the approach is to envelope the shocks of interest. The one warning is to avoid combining shocks with radically different spectral content, as this can make it difficult to implement the resulting combined shock in the lab.

The most common scheme combines two or more axis-specific specifications into a composite specification. The primary benefit of this approach is a reduced chance of the test engineer using the wrong specification for a test. However, this approach should be discouraged because all but one of the directions are being over tested. Therefore, it should not be done without consulting the component designer since there may be a “weak” direction that would have aligned with the lowest of the three axis-specific specifications. Furthermore, some testing schemes can generate responses in multiple directions (such as resonant fixture testing used to replicate a pyroshock environment) but achieving the desired 3-D levels usually benefits from having the correct levels for each direction.

The second method is the combination of parallel environments (i.e., a component can expect to see one of a set of environments but not all of them). The best example is a set of specifications based on three different aircraft. This step is typically implemented at the request of the systems engineer. The recommended technique is based on having the final specification produce as little additional fatigue damage as the highest of the underlying specifications. One means of achieving this goal is to use time compression models to adjust the duration of the specifications so that they are all the same duration and then envelope the specifications. Figure 22 presents an example of this process. This problem was chosen to demonstrate the concept of “decompression”. For frequencies above 400 Hz the duration of the driving ASD was shorter than the selected composite duration so the levels needed to conserve the total fatigue damage was lower.

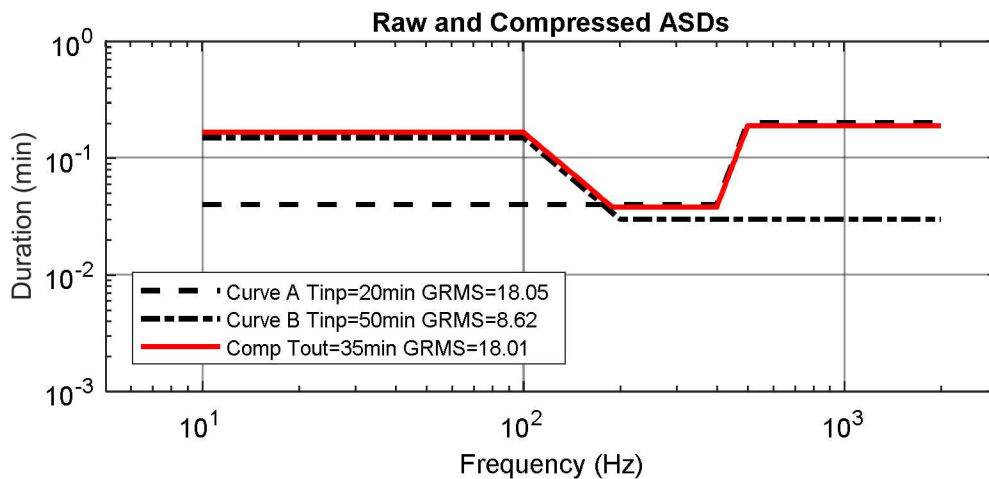


Figure 22: Example of Time Compressed Composite Random Vibration Specification for Parallel Environments

The third scheme involves the combining of serial environments (i.e., environments that the component will experience in sequence). For this class of environments, the goal is to create a specification that produces as much fatigue damage as the sum of the underlying environments. One approach for accomplishing this is to employ a time compression fatigue model to the specifications of interest one frequency at a time. The lower level spectra are increased until they match the highest spectrum. The corresponding test durations are compressed according to the fatigue model. The resultant spectrum will have a different duration associated with each frequency line. At this point the analyst can either 1) keep this preliminary composite spectrum and define the test duration based on the longest of the frequency specific durations, or 2) raise the level of the composite spectrum until the equivalent duration for all frequencies is the same (typically the shortest of the preliminary frequency specific durations). Figure 23 presents the individual and final composite spectra using the latter approach.

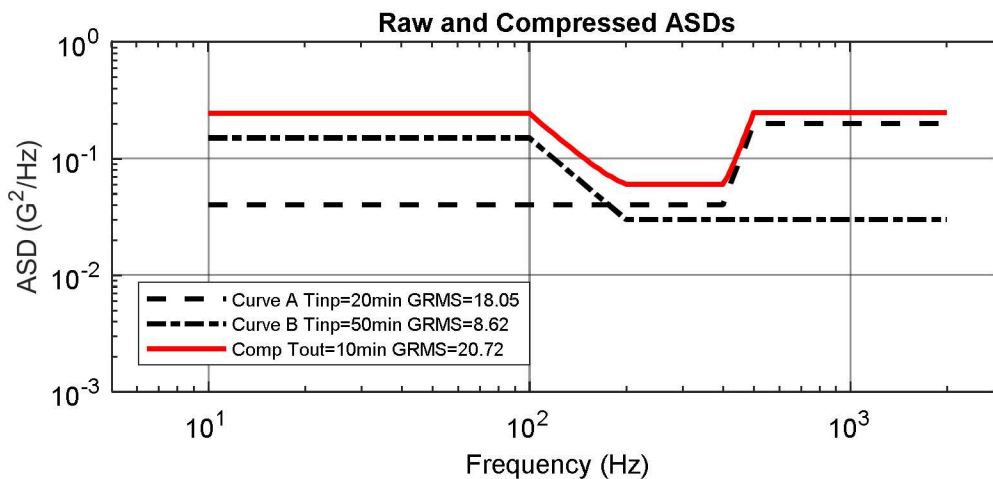


Figure 23: Example of Time Compressed Composite Random Vibration Specification for Serial Environments

One note to the reader regarding these techniques. Time compression models are not perfect so the more one compresses the original durations, the less credible the resulting specification will be. Furthermore, altering the shape of the spectrum will change how a component's resonant modes are excited. Therefore, one should try and only combine specifications having similar durations and spectral content. Similarly, one should only time compress long duration, low magnitude environments and never more than needed to make the lab test practical.

The last topic is the omission benign environments. This should not be done without some form of damage model (preferably one involving a FE model), but at least one that involves the resonant modes of the component. The safest approach is to look for environments that have spectral content well below the lowest resonant frequency (which transportation environments often do). This tends to work in ones favor because those are also the longer duration environments so one gets the most benefit from omitting them.

COMPONENT TESTING ISSUES

The final step in the overall process is the implementation of the test specifications. There are numerous ways in which a test can go wrong, but often trouble can be averted by advanced planning by the component designer, the environments engineer, and the test engineer.

One issue is the upper frequency of the test. Best practices dictate that the specifications initially be defined out to the highest frequency for which the field data can be trusted and/or the response rolls off to negligible levels. However, it must also be recognized that shakers have issues controlling inputs above 2-3 kHz depending on the weight of the test article. Therefore, it may be necessary to truncate a specification or at the very least allow for wider tolerances above the frequency where the shaker dynamics begin to affect the controllability of the test.

The ideal approach is to use an analytical model such as a FE analysis to identify the frequency above which an incremental extension of the spectrum results in little or no increase in the overall stress. Obviously, such a prediction is only as good as the fidelity and resolution of the FE model, but in general a component having a dozen or so significant resonant modes in each axis below a given frequency will not need to be tested above that frequency, and only the very stiffest of components will not meet that criteria for a 3 kHz cutoff frequency.

Another issue is the testing of components having strong resonant behavior. As was discussed in the section on system testing, conducting base excitation tests using straight-line segment specifications will tend to over drive the fixed base resonant frequencies of the component. Applying a response limit during vibration testing based on knowledge of the component's response in the field will notch the input specification at the fixed base resonances in a manner that is similar to what occurs in the field and hence keep the component from being over tested.

If field response data do not exist, the NASA force limited vibration monograph [18] presents models for identifying how deep the notch should be. The NASA models assume that the maximum input force is related to the driving point impedances of the payload and the system. Figure 24 presents one of the NASA models, which assumes that the system, M_1 , and payload, M_2 , can be modeled as a Two Degree of Freedom (TDOF) system. Figure 25 presents an example for a TDOF coupled system

consisting of an 11-lb payload with a 200 Hz resonant frequency and a 1000-lb system with a first resonant mode of 20 Hz. The upper plot in Figure 25 shows the skeleton and dynamic mass lines associated with the driving point impedances for the payload and the skeleton mass line for the system. The middle plot in Figure 25 presents the corresponding raw and notched input ASDs, while the lower plot presents the corresponding response ASDs for the payload.

The two points of interest in this analysis are: 1) notching is justified even though the mass of the payload is much less than the mass of the system (in part because the payload is stiffer), and 2) a 1% reduction in the overall Grms of the input specification results in a significant reduction in the response at the resonant frequency of the payload.

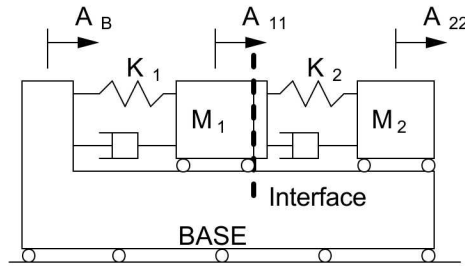


Figure 24: NASA TDOF Force Limiting Model

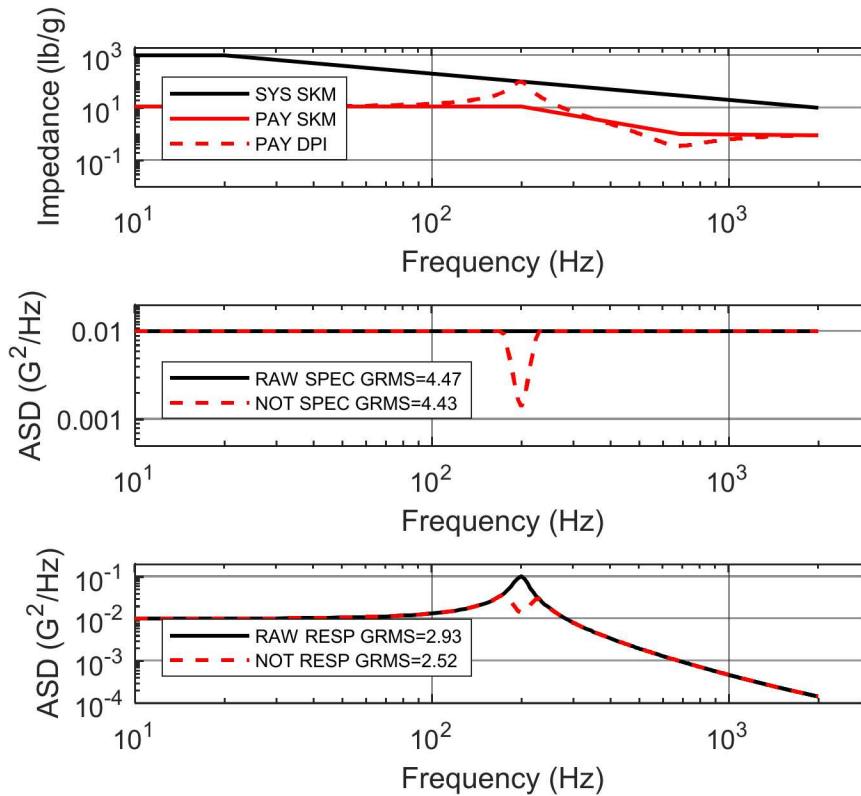


Figure 25: Component Raw and Notched Acceleration Response Spectra

While shaker shocks cannot be actively response limited during the test, it is possible to adjust the input such that the responses of interest is kept within a desired range if one is permitted to measure transfer functions for the test setup ahead of time. One approach incorporates a Single-Input-Multiple-Output (SIMO) optimization scheme directly in the algorithm for synthesizing

the input waveform composed of sums of decayed sinusoids to achieve the desired response at several locations of interest in a least squares sense [20].

The intensity of the input waveform can vary considerably depending on how the tonal frequencies interact with the system resonances. Therefore, when generating the inputs for a SIMO analysis, a Monte Carlo algorithm should be used to generate multiple combinations of tonal frequencies. Figure 26 shows a 3-DOF system consisting of an input and two SDOF oscillators. A set of 20 Monte Carlo SIMO simulations were performed. The one producing the best combination of a low rms dB error and minimum input peak acceleration was chosen. Figure 27 compares the raw and achieved inputs and responses.

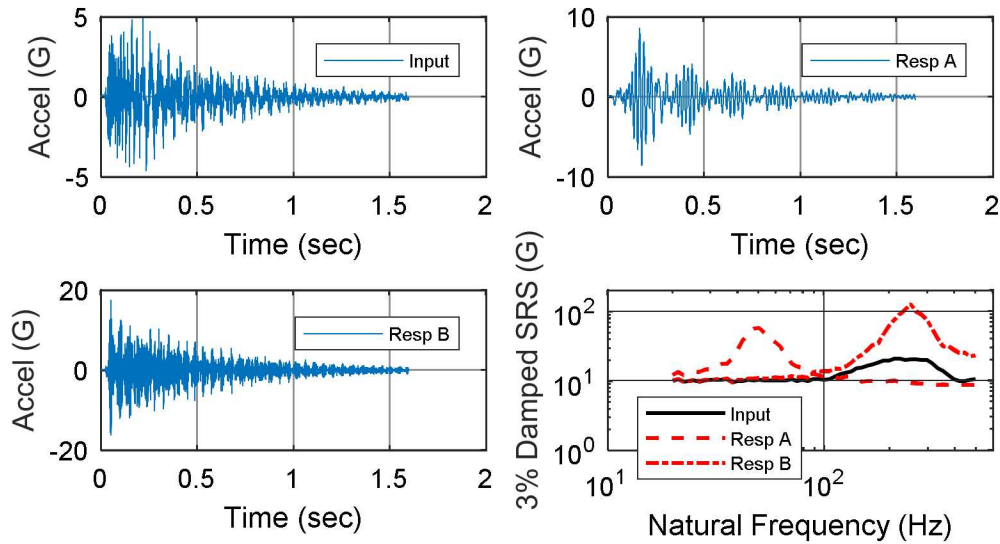


Figure 26: 3-DOF Model for use in SIMO Optimization Example

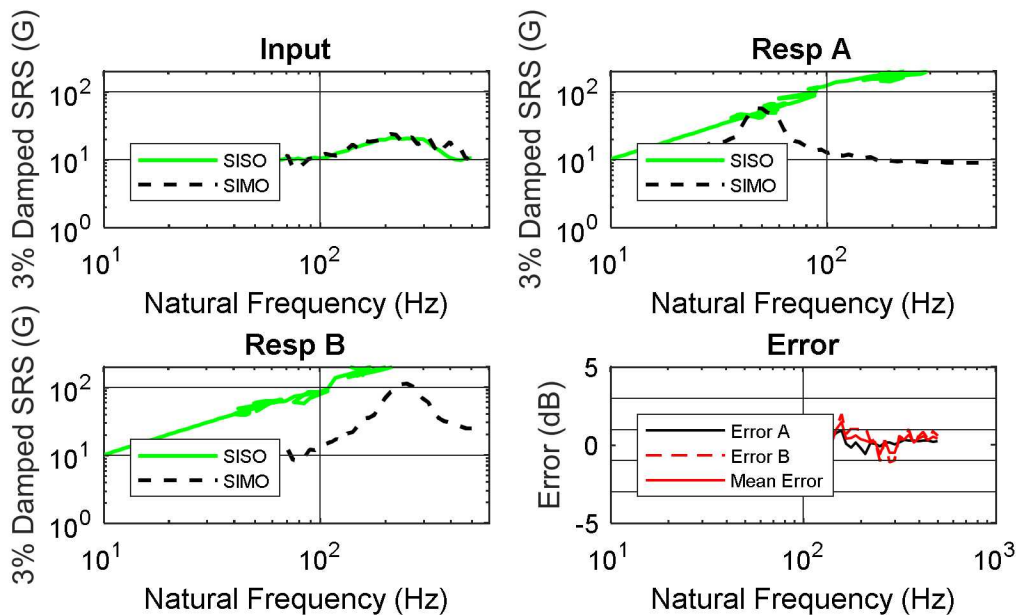


Figure 27: SIMO Shaker Shock Synthesis

One common approach that can result in inconsistent test results is the simultaneous testing of multiple components. Unless the fixture is extremely rigid, this approach will often result in different excitation levels for each component. At the very least the test engineer should monitor the response of each component, but ideally the control scheme should take those responses

into account. Average control has some benefit, but if one needs to ensure each component is exposed to at least the desired levels, then a minimum extremal control scheme should be used.

Ironically, if one of the components is loosely fixtured, the control system will increase the input to bring the levels for that component within spec. This results in the inadvertent over testing of the other components, so it should only be employed for the testing of robust components. Good fixture design is the best defense against this, but response limiting can also be employed (which sort of defeats the purpose of minimum extremal control).

When trying to replicate a shock environment, the best approach is with a shaker owing to the ability to shape the spectral content. The main limitation of shakers is that the peak acceleration levels can only be a few hundred G's, the net velocity and displacement must be within the shaker's capabilities, and the upper frequency limit is 4-6 kHz.

One last comment on shaker shocks pertains to defining the duration. Again, the nature of SRS allows for a wide range of durations for the input acceleration waveform while still producing the desired SRS. Temporal moments [21] have been shown to be useful in producing laboratory shaker shocks that more closely replicate the duration of the field environments.

When shaker shock testing cannot achieve the desired levels and/or spectral content, the test engineer must resort to drop tables and resonant fixtures.

Drop table shock testing is commonly employed owing to the ease of implementation. However, except for environments such as ground impact, which tend to have a significant one-sided acceleration content, the waveform generated by a drop table (a half-sine, haversine, or terminal peak sawtooth) rarely looks like the field environment. The sole criteria for using such a test is the assertion that a test is conservative if the SRS produced by the test exceeds the SRS of the test specification. This puts a lot of pressure on the belief in SRS as being the only possible damage metric. However, drop table testing will continue to be used so the analyst should at least try and achieve the best match for both the SRS and the peak acceleration.

Perhaps the greatest issue with drop table testing is the need to use a long duration and short duration drop shock to span the desired frequency range. Since these shocks must be done sequentially one does not excite the resonant frequencies of the component simultaneously. Figure 28 presents an example of this. The concept of mounting resonant fixtures on the drop table (which would produce a waveform consisting of a low frequency haversine combined with a high frequency ringing waveform) has been studied and such an approach has promise for replacing the need for double haversines.

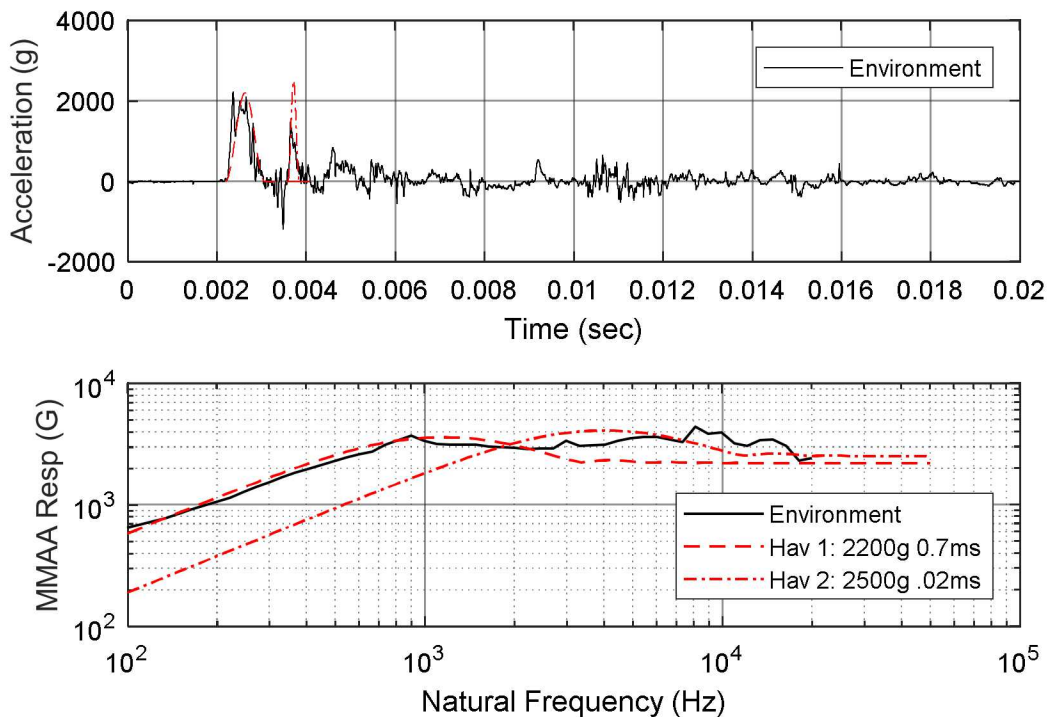


Figure 28: Haversine Drop Shocks for Ground Impact Field Environment

Resonant fixture testing produces oscillatory decaying waveforms that are very similar in nature to many field environments such as pyrotechnically induced shocks. However, the test engineer is limited to a waveform based on the fundamental resonant frequency of the fixture and perhaps some harmonics. Controlling the damping is also somewhat of an art. Therefore, the analyst and component designer must usually work with the test engineer to develop the best possible resonant fixture waveform and then focus on replicating that for the remainder of the test series. Figure 29 presents examples of poor and good resonant fixture tests.

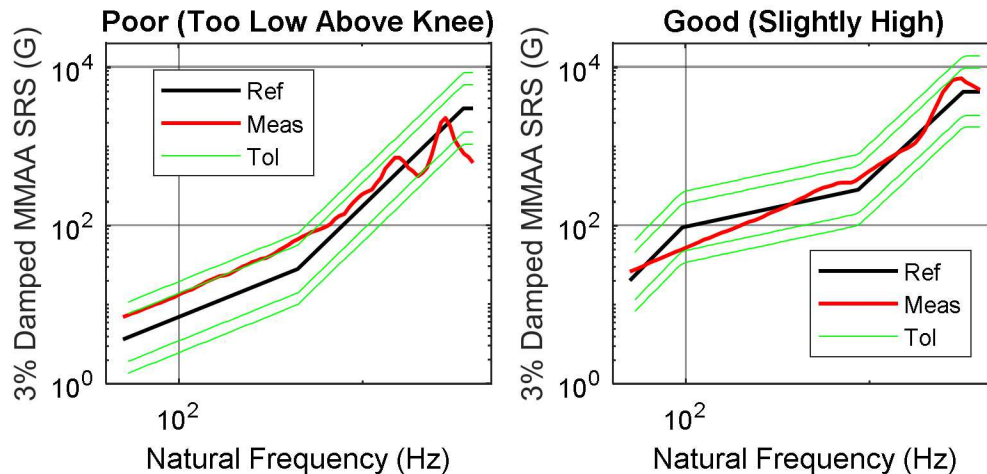


Figure 29: Examples of Resonant Fixture Tests

SUMMARY AND CONCLUSIONS

This paper has covered many topics associated with the processing of field data and the development of laboratory test specifications. Although the topics have been covered at a fairly high level, the author hopes that the reader will appreciate the many concepts that one should consider when developing specifications. The referenced papers provide a more in-depth review of the techniques discussed.

REFERENCES

- [1] Welch, P. D., A Direct Digital Method of Power Spectrum Estimation, IBM Journal, April, 1961.
- [2] Nuttall, A., "Spectral Estimation by Means of Overlapped Fast Fourier Transform Processing of Windowed Data; NUSC Rept. No. 4169, Naval Underwater Systems Center, New London, CT.
- [3] NASA-HDBK-7005, Dynamic Environmental Criteria, December 4, 2000.
- [4] Piersol, Allan G., Optimum Resolution Bandwidth for Spectral Analysis of Stationary Random Vibration Data, Shock and Vibration, Vol. 1, No. 1, pp 33-43 (1993).
- [5] Edwards, Timothy S., "Using Work and Energy to Characterize Mechanical Shock" Proceeding of the 74th Shock and Vibration Symposium, 2003.
- [6] Mil-Std-810G, Environmental Engineering Considerations and Laboratory Tests, 31 October 2008.
- [7] Piersol, A. G., Vibration and Acoustic Test Criteria for Captive Flight of Externally Carried Stores, AFFDL-TR-71-158. DTIC No. AD-893-005L, December 1971.
- [8] Cap, J. S., C' de Baca, M. K., Skousen, T. L.; The Derivation of Maximum Predicted Environments for Externally Carried Stores using a Small Number of Flight Tests; Proceedings of the 84th Shock and Vibration Symposium; November 3-7, 2013; Atlanta, Georgia
- [9] Owen, D. B., "Factors for One-Sided Tolerance Limits and for Variables Sampling Plans," Sandia Monograph SC-R-607, Sandia Corp., Albuquerque, NM, Mar. 1963.
- [10] SMC-TR-06-11, 6 September 2006; Test Requirements for Launch, Upper Stage, and Space Vehicles.
- [11] Pendelton, L. R., and Henrikson, R. L., Flight-to-Flight Variability in Shock and Vibration Levels Based on Trident I Flight Data, Proceedings of the 53rd Shock and Vibration Symposium, Classified Supplement (unclassified paper) 1983.
- [12] Cap, J. S., and Paez, T. L., A Procedure for the Generation of Statistically Significant Transient Signals; Proceedings of the 75th Shock & Vibration Symposium; October 18-22th, 2004; Virginia Beach, VA

- [13] Cap. J. S., An On-Road Shock & Vibration Response Test Series Utilizing Worst Case and Statistical Analysis Techniques; Proceedings of the 68th Shock & Vibration Symposium; November 1997; Baltimore, Md.
- [14] Cap, J. S., C' de Baca, M. K., The Derivation of Appropriate Laboratory Vibration Test Durations and Number of Shock Hits from Non Stationary Field Test Data; Proceedings of the 86th Shock and Vibration Symposium; October 5-8, 2015; Orlando, FL (coauthor: M. C de Baca).
- [15] Cap, J.S., Norman, S., and Smallwood, D. O., The Derivation of Multiple-Input-Multiple Output (MIMO) Acoustic Test Specifications to Simulate a Missile Flight; Proceedings of the 86th Shock and Vibration Symposium; October 5-8, 2015; Orlando, FL
- [16] Rohe D.P., Nelson G.D., Schultz R.A. (2020) Strategies for Shaker Placement for Impedance-Matched Multi-Axis Testing. In: Walber C., Walter P., Seidlitz S. (eds) Sensors and Instrumentation, Aircraft/Aerospace, Energy Harvesting & Dynamic Environments Testing, Volume 7. Conference Proceedings of the Society for Experimental Mechanics Series. Springer, Cham.
- [17] Cap, J. S; A Technique for the Identification of the Optimum Inputs for a Vibration or Acoustic Test; Proceedings of the 76th Shock & Vibration Symposium; October 31st – November 3rd, 2005; Destin, FL.
- [18] NASA document RP-1402, Force Limiting Vibration Testing Monograph.
- [19] Smallwood, David O., Methods Used to Match Shock Spectra Using Oscillatory Transients; Proceedings of the Institute of Environmental Sciences, 1974, pp490-420.
- [20] Heitman, Chad, Cap, J.S., Murphy, Dylan; Monte Carlo Optimization of a Single Input Multiple Output (SIMO) Input Derivation for an Oscillatory Decaying Shock, ; Proceedings of the 87th Shock and Vibration Symposium; New Orleans, LA.
- [21] Cap, J. S., and Smallwood, D. O.; Characterization of Ignition Overpressure Using Band Limited Temporal Moments; Proceedings of the 65th Shock & Vibration Symposium; October 31-November 3, 1994; San Diego CA.,